

Invited Lecture at the  
Acoustical Society of America Meeting, June 2007, Salt Lake City, Utah

## BUBBLY CLOUD DYNAMICS AND CAVITATION

Christopher E. Brennen  
California Institute of Technology,  
Pasadena, California 91125

### Abstract

In many cavitating liquid flows, when the number and concentration of the bubbles exceeds some critical level, the flow becomes unsteady and large clouds of cavitating bubbles are periodically formed and then collapse when convected into regions of higher pressure. This phenomenon is known as cloud cavitation and when it occurs it is almost always associated with a substantial increase in the cavitation noise and the potential for material damage associated with the cavitation. These increases represent serious problems in devices as disparate as marine propellers, cavitating pumps and artificial heart valves. This lecture will present examples of the phenomenon and review recent advances in our understanding of the dynamics and acoustics of clouds of bubbles and cloud cavitation. Both analyses of these complex multiphase flows and experimental observations will be used to identify the key features of the phenomenon and the parameters that influence it.

### 1 Introduction

It has become abundantly clear in recent years that knowledge of the dynamics and acoustics of bubble clouds (as opposed to single bubbles) is essential to our understanding of a very broad range of physical

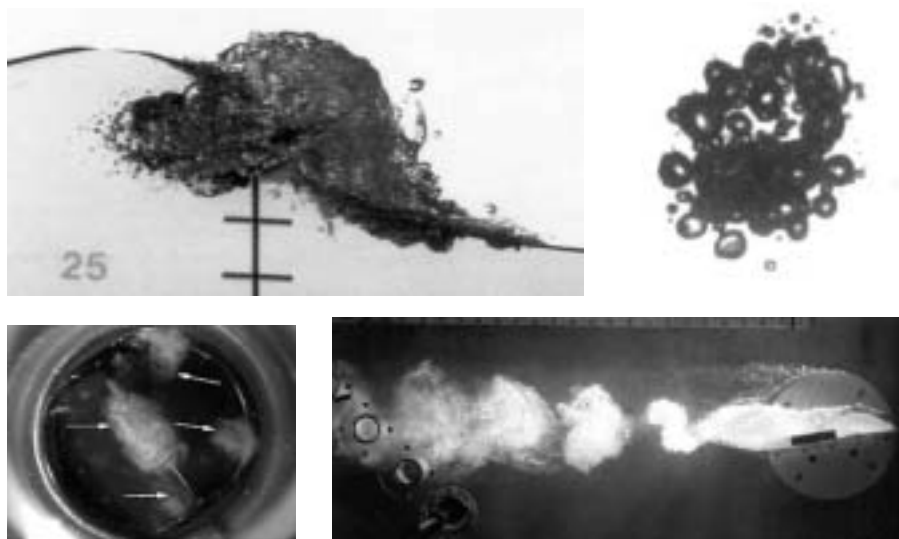


Figure 1: Examples of bubble clouds: Clockwise from upper left: a breaking wave (Petroff 1993), a cloud formed after collapse of a vapor bubble (Frost and Sturtevant 1986), clouds formed in the wake of an oscillating hydrofoil, clouds formed downstream of an artificial heart valve closure (Rambod *et al.* 1999).

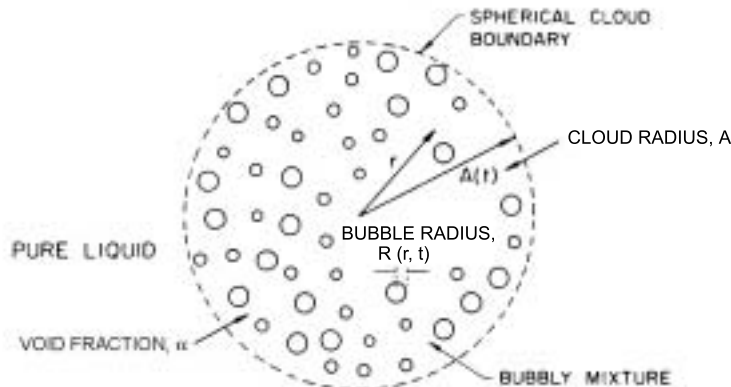


Figure 2: Spherical cloud of bubbles: notation.

effects involving bubbles. For example, the collapse of clouds of cavitation bubbles often results in much greater noise and damage than would result from the sum of the effects of individual bubbles. In some contexts such as with cavitating propellers or turbomachines this is a cause for grave concern and a lack of understanding of the processes of periodic formation and collapse of cavitation clouds remains a key issue. Similar concerns surround the formation of clouds of cavitation bubbles in contexts as diverse as artificial heart valves or the earthquake-induced cavitation effects on dams. But there are also contexts in which we can take advantage of these cloud effects such as in the destruction of kidney stones by lithotripsy.

In this paper we shall not attempt a comprehensive review of the multitude of contexts in which bubble cloud dynamics and acoustics are important (the few examples shown in figure 1 will suffice to demonstrate the ubiquity of bubble clouds). Rather, this review will be confined to a brief description of our current understanding of the mechanics of the cloud effects, of the limitations in our ability to model these processes as well as a description of some experiments designed to look for some of the key phenomena.

## 2 Review of bubble cloud effects

Though the first analysis that indicated how bubbles might behave collectively was conducted by van Wijngaarden (1964) on a plane layer of bubbles next to a wall, it is more convenient to focus attention on a simple spherical cloud surrounded by pure liquid and to briefly review the dynamics and acoustics of such a cloud. Initially, it will be assumed as indicated in figure 2 that all the bubbles in the cloud have the same equilibrium size,  $R_0$ , and that they are uniformly distributed within the cloud so that the population as represented by the initial equilibrium void fraction,  $\alpha_0$ , is uniform within the cloud. Radial position within the cloud is denoted by  $r$  and the initial radius of the cloud by  $A_0$ .

### 2.1 Natural frequencies of a spherical cloud

We begin by reviewing the linear dynamics of such a cloud as first analysed by d'Agostino and Brennen (1983, 1989). A simple linear analysis that assumes an incompressible liquid reveals that the cloud has an infinite set of natural frequencies and modes. The natural frequencies,  $\omega_n$ , are given by

$$\omega_n = \omega_N \left[ 1 + \frac{4}{3\pi^2(2n-1)^2} \frac{A_0^2}{R_0^2} \frac{\alpha_0}{1-\alpha_0} \right]^{-\frac{1}{2}} ; n = 1, 2, \dots \quad \text{and} \quad \omega_\infty = \omega_N \quad (1)$$

where  $\omega_N$  is the natural frequency of an individual bubble in an infinite liquid. The above is an infinite series of frequencies of which  $\omega_1$  is the lowest. The higher frequencies approach  $\omega_N$  as  $n$  tends to infinity. As expected these natural frequencies correspond to modes with more and more nodes as  $n$  increases (see Brennen 1995). Note in particular that the lowest natural frequency,  $\omega_1$ ,

$$\omega_1 = \omega_N \left[ 1 + \frac{4}{3\pi^2} \frac{A_0^2}{R_0^2} \frac{\alpha_0}{1 - \alpha_0} \right]^{-\frac{1}{2}} \quad (2)$$

can be much smaller than the individual bubble frequency,  $\omega_N$ .

Indeed the natural frequencies of the cloud will extend to frequencies much smaller than  $\omega_N$ , if the initial void fraction,  $\alpha_0$ , is much larger than the square of the ratio of bubble size to cloud size ( $\alpha_0 \gg R_0^2/A_0^2$ ). If the reverse is the case ( $\alpha_0 \ll R_0^2/A_0^2$ ), all the natural frequencies of the cloud are contained in a small range just below  $\omega_N$ . This defines a special parameter,  $\beta = \alpha_0 A_0^2/R_0^2$ , that governs the cloud interaction effects and which we term the ‘‘Cloud Interaction Parameter’’. If  $\beta \ll 1$  there is relatively little bubble interaction effect and all the bubbles oscillate at close to the frequency,  $\omega_N$ , as if each were surrounded by nothing but liquid. On the other hand when  $\beta > 1$  the cloud has natural frequencies much less than  $\omega_N$  and there are strong interaction effects between the bubbles in the cloud. Note that in various applications the magnitude of  $\beta$  could take a wide range of values from much less than unity to much greater than unity. It will be small in small clouds with a few large bubbles and a low void fraction but could be large in large clouds of small bubbles with higher void fraction.

## 2.2 Linear response of a spherical cloud to forced vibration

It is also valuable to explore the linear response of a cloud to forced vibration induced when the pressure in the liquid far from the bubble is set to oscillate at some frequency,  $\omega$ . The linear response of the cloud at various frequencies can be illustrated by plotting the amplitude of bubble radius oscillations against the radial position within the cloud,  $r/A_0$ . An example for the case of  $\beta \approx 0.8$  is shown in figure 3 taken from d’Agostino and Brennen (1989). For frequencies  $\omega < \omega_N$  such as the upper two curves in figure 3 the entire cloud responds in a fairly uniform manner. However when  $\omega$  is increased to a value greater than but close to  $\omega_N$  (such as the dotted line), only a surface layer of bubbles exhibit significant near-resonant response. The core of the cloud is essentially shielded by the response of that outer layer. With further increase in the frequency well above  $\omega_N$  the response evens out again. These variations within the cloud become less and less pronounced as  $\beta$  is decreased.

Typical information on the magnitude of the response at different frequencies is shown in more detail in figure 4, where the amplitude of bubble radius oscillation at the cloud surface is presented as a function of  $\omega$ . The solid line corresponds to the result obtained without any bubble damping. Consequently, there are asymptotes to infinity at each of the cloud natural frequencies; for clarity we have omitted the numerous asymptotes that occur just below the bubble natural frequency,  $\omega_N$ . Also shown in this figure are the corresponding results when a reasonable estimate of the damping is included in the analysis (d’Agostino and Brennen 1989). The attenuation due to the damping is much greater at the higher frequencies so that, when damping is included the dominant feature of the response is the lowest natural frequency of the cloud,  $\omega_1$ . The response at the bubble natural frequency,  $\omega_N$ , becomes much less significant.

The effect of varying the cloud interaction parameter,  $\beta$ , is shown in figure 5, where the amplitude of bubble radius oscillation at the cloud surface is presented as a function of  $\omega$ . Note that increasing  $\beta$  causes a reduction in both the amplitude and frequency of the dominant response at the lowest natural frequency of the cloud. d’Agostino and Brennen (1988) have also calculated the acoustical absorption and scattering cross-sections of the cloud that this analysis implies. Not surprisingly, the dominant peaks in the cross-sections occur at the lowest cloud natural frequency.

It is important to emphasize that the results presented above are linear and that there are very significant nonlinear effects that we now proceed to describe. In addition we have focused exclusively on spherical bubble clouds since solutions of the basic equations for other, more complex geometries are not readily obtained.

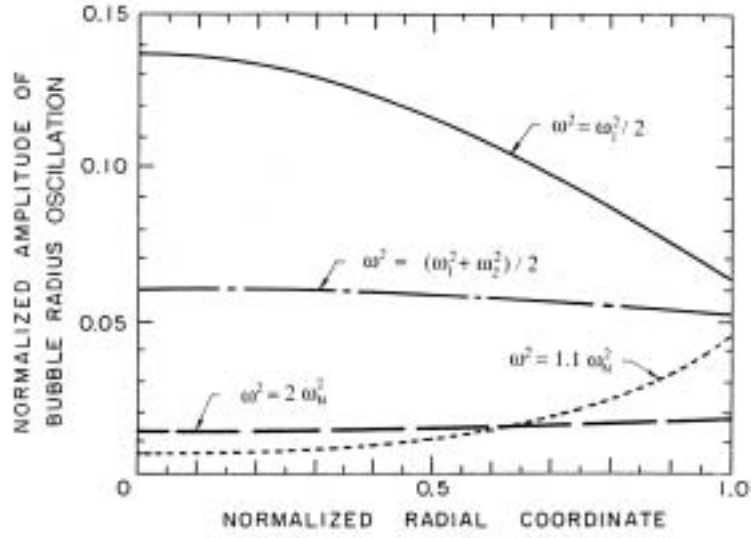


Figure 3: The distribution of bubble radius oscillation amplitudes within a cloud subjected to forced excitation at various frequencies,  $\omega$ , as indicated (for the case of  $\beta \approx 0.8$ ). From d'Agostino and Brennen (1989).

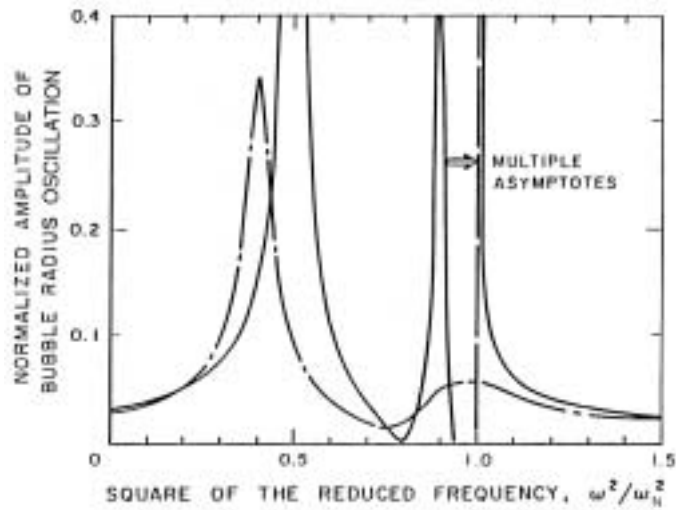


Figure 4: The amplitude of the bubble radius oscillation at the cloud surface as a function of frequency (for the case of  $\beta \approx 0.8$ ). Solid line is without damping; broken line includes damping. From d'Agostino and Brennen (1989).

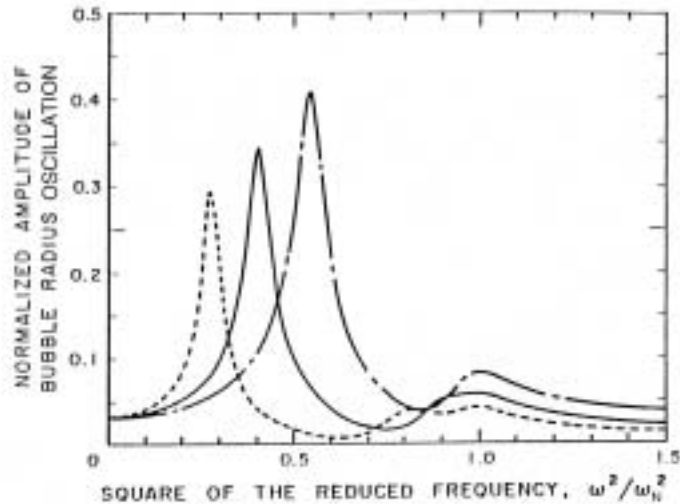


Figure 5: The amplitude of the bubble radius oscillation at the cloud surface as a function of frequency for damped oscillations at three values of  $\beta \approx 0.8$  (solid line),  $\beta \approx 0.4$  (dot-dash line), and  $\beta \approx 1.65$  (dashed line). From d’Agostino and Brennen (1989).

However, d’Agostino et al. (1988) have examined some of the characteristics of this class of bubbly flows past slender bodies (for example, the flow over a wavy surface). Clearly, in the absence of bubble dynamics, one would encounter two types of flow: subsonic and supersonic. Interestingly, the inclusion of bubble dynamics leads to three types of flow. At sufficiently low speeds one obtains the usual elliptic equations of subsonic flow. When the sonic speed is exceeded, the equations become hyperbolic and the flow supersonic. However, with further increase in speed, the time rate of change becomes equivalent to frequencies above the natural frequency of the bubbles. Then the equations become elliptic again and a new flow regime, termed “super-resonant,” occurs. d’Agostino et al. (1988) explore the consequences of this and other features of these slender body flows.

### 2.3 Cavitation of a spherical cloud

If a spherical cloud is subjected to an episode of sufficiently low pressure it will cavitate, in other words the bubbles will grow explosively to many times their original size. Subsequently, if the pressure far from the cloud increases again (as, for example, when the cloud is convected out of the region of low pressure) the bubbles will collapse violently. The reaction of a single bubble to such a low pressure episode has, of course, been studied extensively; typically the Rayleigh-Plesset equation is used to model the highly non-linear reaction of the single bubble. However, the response of a cloud of bubbles is more complex and requires the use of continuity and momentum equations coupled to the Rayleigh-Plesset equation in order to model the two-phase flow within the cloud. Here we briefly review the calculations of Wang and Brennen (1995a, b) and Reisman *et al* (1998), who numerically solved such a set of equations in order to uncover the dynamics of a spherical cloud of cavitating bubbles. Previous numerical investigations of the nonlinear dynamics of cavity clouds were carried out by Chahine (1982), Omta (1987), and Kumar and Brennen (1991, 1992, 1993). One interesting phenomenon that emerges from Kumar and Brennen is the interaction between the bubbles of different size that would commonly occur in any real cloud. The phenomenon, called “harmonic cascading” (Kumar and Brennen 1992), occurs when a relatively small number of larger bubbles begins to respond nonlinearly to some excitation. Then the higher harmonics produced will excite the much larger number of smaller bubbles at their natural frequency. The process can then be repeated to even smaller bubbles. In essence, this nonlinear effect causes a cascading of fluctuation energy to smaller bubbles and

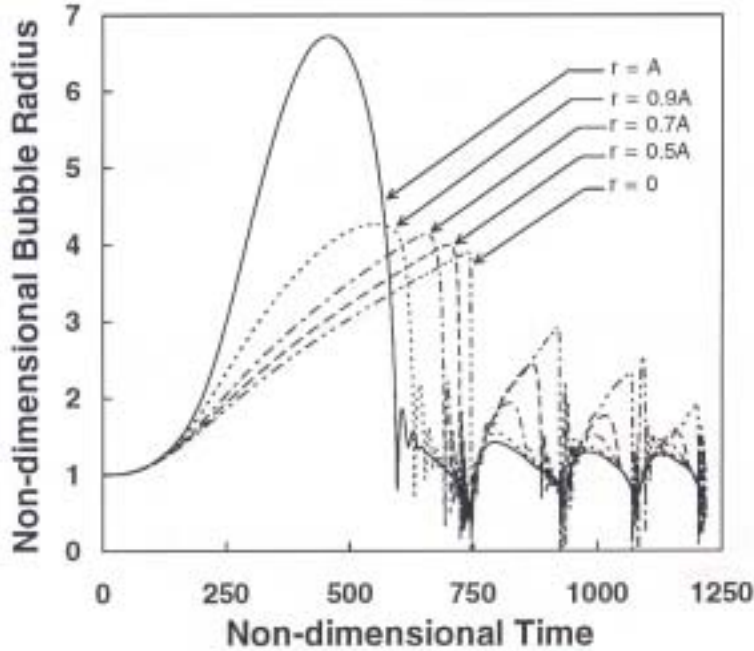


Figure 6: A typical time history of the bubble size at six different Lagrangian positions in a spherical cloud in response to an episode of reduced pressure in the surrounding liquid (between  $t=0$  and  $t=250$ ). These results for a parameter  $\beta$  that is much greater than unity. From Wang and Brennen (1995).

higher frequencies.

But we focus here on the non-linear calculations of the growth and collapse of a spherical cloud of bubbles by Wang and Brennen (1995a, b) and Reisman *et al* (1998). It transpires that the response of a cloud to an episode of reduced pressure in the surrounding liquid is quite different depending on the magnitude of  $\beta$ . When  $\beta$  is much greater than unity the typical cloud response to an episode of reduced pressure is shown in Figure 6. Note that the bubbles on the surface of the cloud grow more rapidly than those in the interior which are effectively shielded from the reduced pressure in the surrounding liquid. More importantly the bubbles on the surface collapse first and a collapse front propagates inward from the cloud surface developing into a substantial shock wave.

Figure 7 is a snapshot in time of the form of the collapse front and the large pressure pulse or shock wave that is associated with it. Due to geometric focusing this shock wave strengthens as the shock proceeds inwards and creates a very large pressure pulse when it reached the center of the cloud. On the other hand when  $\beta$  is small, the response of the cloud is quite different as shown in Figure 8. Then the shielding causes the bubbles at the center of the cloud to collapse first, resulting in an outgoing collapse front that weakens geometrically resulting in a quite different dynamic.

While real bubble clouds are often far from spherical the potential for similar shielding effects still clearly exists and later we will describe some experimental observations of shocks in collapsing bubble clouds. It should also be noted that this simple spherical cloud example demonstrates a clear need for enhanced computational tools that would be capable of predicting these effects in more complex geometries. Hence there is a need for CFD methodologies capable of predicting these complex bubbly flows. An example is the work of Tanguay and Colonius (2002) who have simulated the dynamics of the cloud of bubbles formed at the focus of a shock wave lithotripter. Other examples of the development of these codes include the work of Kubota *et al* (1992), Colonius *et al* (1998) and Brennen *et al* (1998).

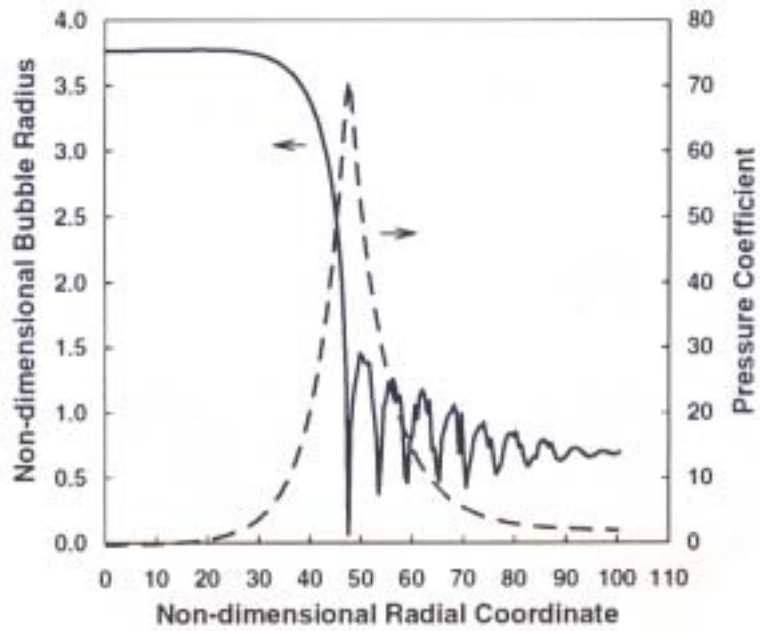


Figure 7: A snapshot in time of the radial distribution of bubble size and pressure from the same calculation as Figure 6 at a moment when the collapse shock is roughly half way into the cloud. From Wang and Brennen (1995).

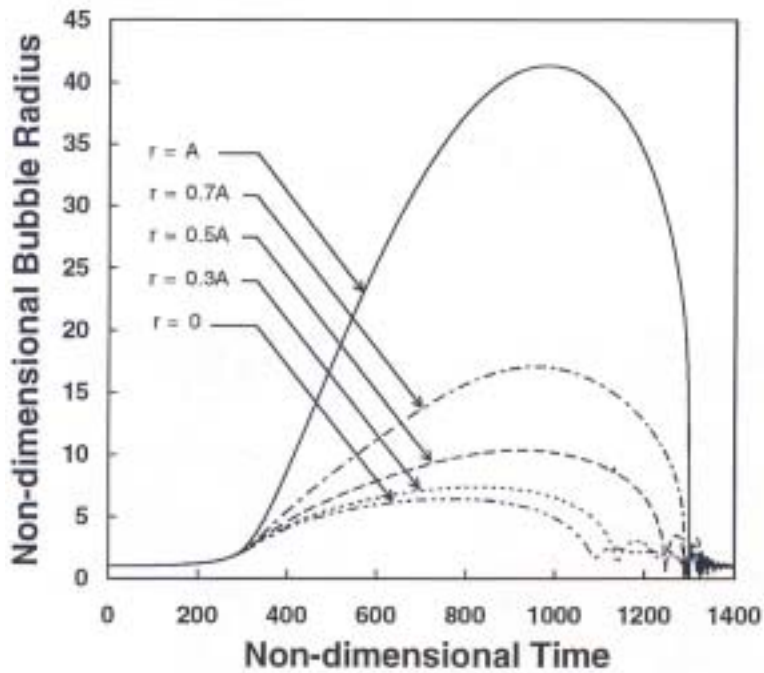


Figure 8: A typical time history similar to that of Figure 6 except that the parameter  $\beta$  is of order unity or less. From Wang and Brennen (1995).

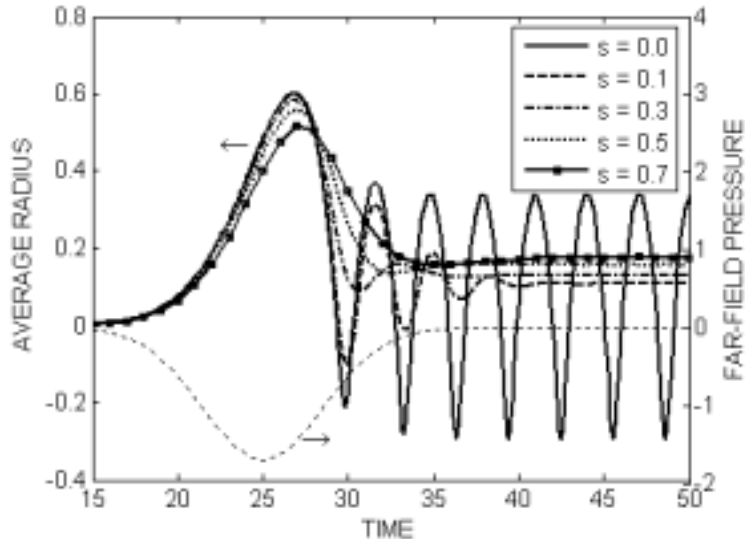


Figure 9: Bubble cloud radius responses to an episode of low pressure (between  $t = 0$  and  $t = ???$ ) for a single equilibrium size cloud ( $s = 0$ ) and clouds with a distribution of bubble size as defined by the non-zero values of the standard deviation,  $s$ . From Ando *et al.* (2007).

## 2.4 The effect of a distribution of bubble sizes

All of the above analyses were confined to clouds of bubbles in which all of the bubbles have the same equilibrium radius and the same natural frequency. Consequently they are disposed to oscillate in unison, for example in the rear of the shock wave displayed in figure 7. Most natural clouds consist of bubbles with a range of equilibrium radii and natural frequencies and it is therefore appropriate to ask whether and how the phenomena described above might be altered by this characteristic. Clearly the computation of the non-linear response of a cloud with multiple bubble sizes is very involved so, not surprisingly, the answer to this question is, as yet, incomplete. However, two pieces of the puzzle are available.

First, Wang (1999) has computed the nonlinear response of a spherical cloud with a simple quartic distribution of bubble sizes. For the set of chosen parameters of his calculations Wang found that a distribution of bubble sizes evens out the oscillations behind the shock that are exhibited in figure 7 and somewhat reduces the magnitude of the associated pressure pulse. He also found that, in a low  $\beta$  case, a distribution could alter the mode of cloud collapse from that of an outgoing wave to that of an ingoing shock wave.

Second, Ando *et al.* (2007), as a part of a wider investigation of the effects of a distribution of equilibrium bubble sizes on the dynamics of a bubbly flow, have examined the combined or integral effects of a distribution of bubble sizes on the dynamics of a dilute cloud in which the effective  $\beta$  is so small that the interaction effects are minimal. In this low  $\beta$  limit the overall cloud dynamics become the summation of the displacement effects of all individual bubble sizes. Using a log-normal bubble size distribution whose width is characterized by the standard deviation,  $s$ , Ando *et al.* have calculated the non-linear response of a spherical cloud to an episode of low pressure. Figure 9 compares the bubble cloud radius response for a range of standard deviations from  $s = 0$  (single equilibrium bubble size) to a broad range of sizes as represented by  $s = 0.7$ . Note that the initial growth of the cloud is not greatly different in each of the five cases but that the subsequent cloud radius oscillations are essentially eliminated by having a distribution of bubble sizes. Consequently the effect of a distribution of size is not greatly different from the effect of additional damping. Notice also from figure 9 that there is a significant long term non-linear effect on the mean cloud size; though the cloud radius is not oscillating, the cloud size is effectively increased by the bubble oscillations going on within the cloud. These results are consistent with those of Wang (1999).

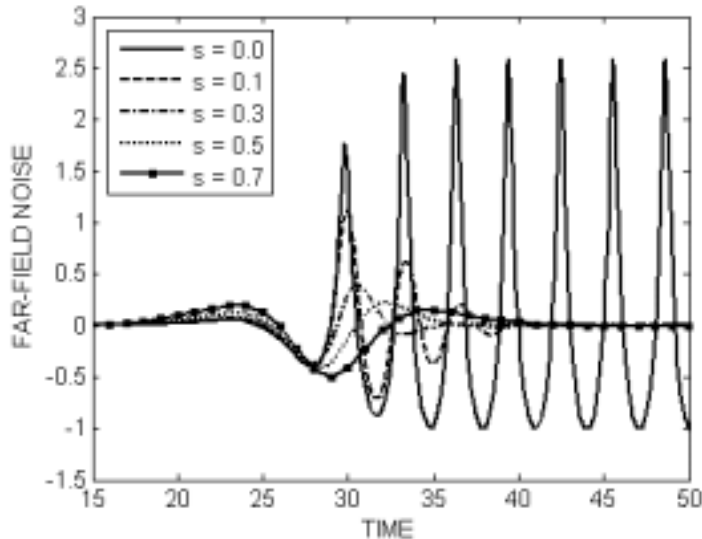


Figure 10: Far-field radiated noise from the bubble clouds of figure 9. From Ando *et al.* (2007).

The effect of these dynamics on the far-field noise radiated by the cloud is shown in figure 10. Again, the large oscillations in the single-bubble-size cloud are effectively eliminated by the presence of a distribution of bubble sizes. In addition the magnitude of the initial pulse in the far-field noise is significantly reduced. We would therefore expect that in a real bubble cloud with substantial variation in the bubble size, the far-field noise would consist of a significant single pulse and little else; moreover the magnitude of that single pulse would be significantly smaller than we might expect based on single-bubble-size analyses. It remains to be determined how these effects might be changed at higher values of  $\beta$ .

### 3 Experimental Observations

#### 3.1 Past Observations

The highly destructive consequences of cloud cavitation have been known for a long time and have been documented, for example, by Knapp (1955), Bark and van Berlekom (1978) and Soyama *et al.* (1992). The generation of these cavitation clouds may occur naturally as a result of the shedding of bubble-filled vortices, or it may be the response to a periodic disturbance imposed on the flow. Common examples of imposed fluctuations are the interaction between rotor and stator blades in a pump or turbine and the interaction between a ship's propeller and the non-uniform wake created by the hull. As a result numerous investigators (for example, Wade and Acosta 1966, Bark and van Berlekom 1978, Shen and Peterson 1978, 1980, Bark 1985, Franc and Michel 1988, Hart *et al.* 1990, Kubota *et al.* 1989, 1992, Le *et al.* 1993, de Lange *et al.* 1994) have studied the complicated flow patterns involved in the production and collapse of cloud cavitation on a hydrofoil. The radiated noise produced is characterized by pressure pulses of very short duration and large magnitude. These pressure pulses were measured by Bark (1985), Bark and van Berlekom (1978), Le *et al.* (1993), Shen and Peterson (1978, 1980) and McKenney and Brennen (1994).

A valuable perspective on the subject of collapsing clouds was that introduced by Mørch (1980, 1981, 1982) and Hanson, Kedrinskii and Mørch (1981). They suggested that the collapse of a cloud of bubbles involves the formation and inward propagation of a shock wave and that the geometric focusing of this shock at the center of cloud creates the enhancement of the noise and damage potential associated with cloud collapse. The aforementioned calculations of Wang and Brennen confirmed these suggestions and identified

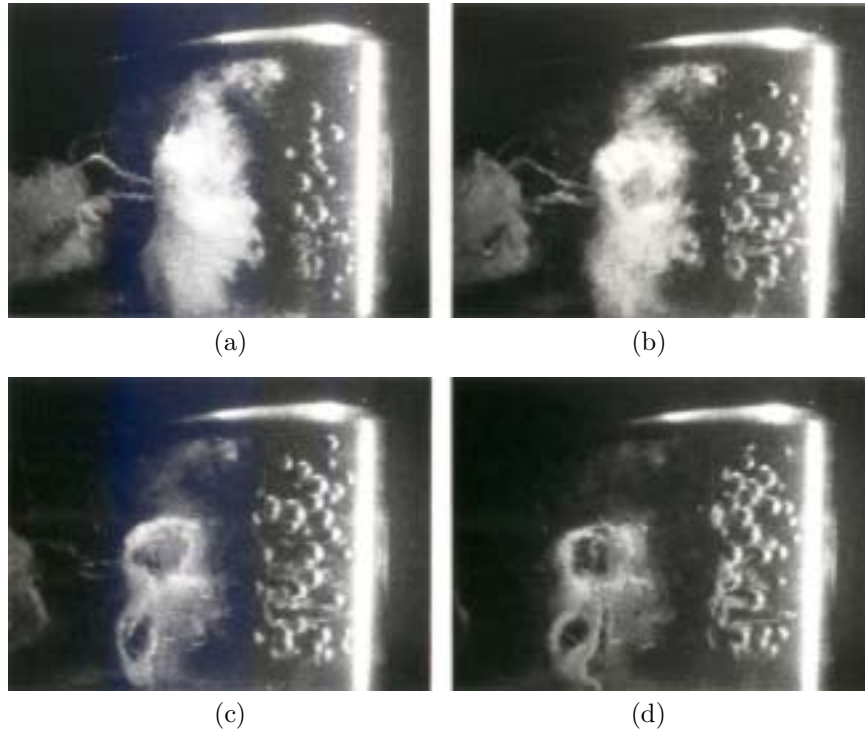


Figure 11: Example of consecutive high speed movie frames ( $2ms$  apart) of the collapse of a cloud of cavitation bubbles on the suction surface of a hydrofoil. The flow is from right to left. A global cloud collapse occurs between frames (b) and (c). From Reisman *et al.* (1998).

the parametric conditions under which those shock waves would arise.

### 3.2 Some experimental observations using an oscillating hydrofoil

We will focus here on the experimental observations of Reisman *et al.* (1998) who deployed an oscillating hydrofoil in a water tunnel to produce regular clouds of cavitation whose behavior could be observed and measured. The experiments were conducted in the Low Turbulence Water Tunnel (LTWT) at Caltech. Several finite span hydrofoils with a rectangular planform, a chord of  $15.8cm$  and a span of  $17.8cm$ , were reflection-plane mounted in the floor of the test section and, as described in Reisman *et al.* (1998), were driven in an oscillatory pitching motion with frequencies up to  $50Hz$  and incidence angle amplitudes of the order of  $5 - 10^\circ$ . One of the hydrofoils was equipped with flush-mounted surface pressure transducers located at 26% span from the foil base and 30%, 50%, 70% and 90% chord from the leading edge (denoted respectively by #1 through #4). Additional dynamic transducers were located on the nearby tunnel walls.

High speed motion pictures (taken at  $500fps$ ) allowed examination of the processes of formation, growth and collapse of a cloud of cavitation bubble during each cycle of the hydrofoil oscillation. During the part of the oscillation cycle when the incidence angle is increasing, cavitation inception occurs in the tip vortex and is soon followed by traveling bubble cavitation on the suction surface. As the angle of attack increases further, the bubbles coalesce into a single attached cavitation sheet; near the end of this process, a re-entrant liquid jet penetrates the attached cavity from downstream and causes the break-up into a cloud of bubbles. This cloud then detaches from the hydrofoil and collapses catastrophically as it is being convected downstream. All of the substantial radiated noise occurred during this bubbly part of the cycle. It consisted of pressure pulses of very short duration and large magnitude that were qualitatively similar to those measured by Bark (1985), Bark and van Berlekom (1978), Le *et al.* (1993) and Shen and Peterson (1978, 1980).

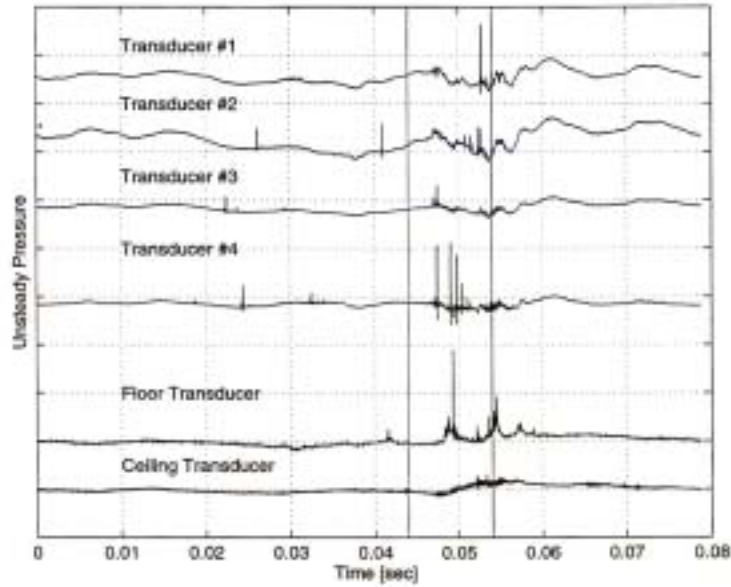


Figure 12: Typical signals from the transducers during a single cycle of foil oscillation. The vertical scale is  $1 \text{ MPa/div.}$  for the hydrofoil surface transducers, #1-#4, and  $100 \text{ kPa/div.}$  for the floor and ceiling transducers. From Reisman *et al.* (1998).

This so-called "global" collapse is illustrated by the four successive movie frames included in figure 11. The global cloud collapse occurs between frames (b) and (c). Note that this collapse results in only a slight change in the cloud radius but a large change in the void fraction magnitude and distribution inside the cloud, an observation that is consistent with the previously described calculations of Wang and Brennen.

Reisman *et al.* (1998) correlated the movies with the transducer pressure measurements and found that the pressure pulses recorded (both on the foil surface and in the far field) were clearly associated with specific structures (more precisely, the dynamics of specific structures) which are visible in the movies. Indeed, it appears that several types of propagating structures (shock waves) are formed in the collapsing cloud and dictate the dynamics and acoustics of collapse.

A typical set of transducer recordings is shown in figure 12 which represents a single foil oscillation cycle with the origin corresponding to the maximum angle of attack. The signals are characterized by very large amplitude pressure pulses with magnitudes of the order of tens of atmospheres and typical durations of the order of tenths of milliseconds. Note that the radiated, far-field acoustic pressure recorded by the floor and ceiling transducers also contains pulses and these are exemplified by the bottom trace in figure 12. The magnitude of the pulses measured by the transducer in the tunnel floor is on the order of one atmosphere. [The low frequency variation present in the signal prior is the result of stresses and accelerations of the hydrofoil rather than pressure variations.]

In the present experiments, two different types of pressure pulses were identified and can be illustrated by figure 12. The pulses occurring before the  $0.04\text{s}$  mark are randomly distributed in time and space and are not repeated from cycle to cycle. These will be referred to as *local* pulses. On the other hand, the pulses located between  $0.04\text{s}$  and  $0.05\text{s}$  occur virtually simultaneously, are of higher amplitude and are repeated each cycle. These will be referred to as *global* pulses; they produced substantial far-field noise. These global pulses were readily correlated with the visual observations of the coherent global collapse of the well-defined bubble cloud described above.

But, unexpectedly, two other types of structures were observed. Typically, their pulses are recorded by

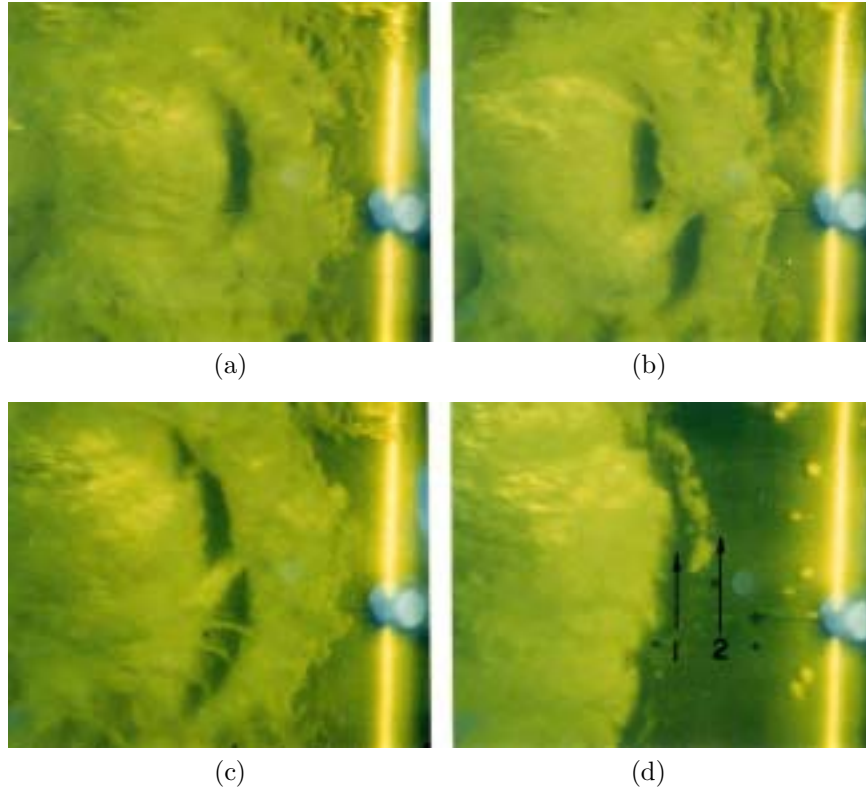


Figure 13: Local pulse structures in the cavitation on the suction surface of a cavitating foil. The flow is from right to left. Crescent-shaped structures are seen in (a), (b), and (c) and a leading edge event with two collapses is shown in photograph (d). From Reisman *et al.* (1998).

only one transducer as exemplified by the individual pulses in figure 12 occurring before the  $0.04s$  mark. These are randomly distributed in time and space and are not repeated from cycle to cycle. They are referred to as *local* pulses. (In contrast the global pulses located between  $0.04s$  and  $0.05s$  occur virtually simultaneously, are of higher amplitude and are repeated each cycle.) While these *local* events are smaller and therefore produce less radiated noise, the pressure pulse magnitudes are almost as large as those produced by *global* events.

Correlation of the high-speed movies with the transducer output revealed that local pulses occurred when one of two particular types of flow structures passed over the face of the transducer. The two types of structures will be referred to as “crescent-shaped regions” and “leading edge structures”; both occur during the less coherent collapse of clouds. Crescent-shaped regions are illustrated in photographs (a) through (c) of figure 13) and careful correlation revealed that the passage of one of these over an individual transducer produced a large local pulse in the output of that transducer. A crescent-shaped region has a low void fraction and, consequently, must involve a substantial compression pulse at its leading edge. These crescent-shaped regions appear randomly and ephemerally in the bubbly mixture. A close look at photograph (c) shows how complicated these flow structures can be since this crescent-shaped region appears to have some internal structure. Photographs (b) and (c) show that more than one crescent-shaped structure can be present at any moment in time.

In addition, the movie and pressure data consistently displayed a local pulse when the upstream boundary, or leading edge, of the detached bubbly mixture passed over a transducer. This second type of local flow structure is illustrated in photograph (d) of figure 13 and also produces a local pulse. These “leading edge

structures” are created when the mixture detaches from the foil; they propagate downstream faster than the mixture velocity.

Parenthetically, we note that injection of air into the cavitation on the suction surface can substantially reduce the magnitude of the pressure pulses produced (Ukon 1986, Arndt *et al.* 1993, Reisman *et al.* 1997). However Reisman *et al.* (1997) have shown that the bubbly shock wave structures still occur; but with the additional air content in the bubbles, the pressure pulses are greatly reduced.

Finally we note that pulses like those measured on the surface of the hydrofoil with typical magnitudes as large as  $10\text{bar}$  and durations of the order of  $10^{-4}\text{s}$  are certainly sufficient to explain the enhanced noise and cavitation damage associated with cloud cavitation. For example, the large impulsive surface loadings due to these pulses could be responsible for the foil damage reported by Morgan (1995), who observed propeller blade trailing edges bent away from the suction surface and toward the pressure surface.

## 4 Concluding Comments

In this paper we have summarized some of the recent advances in our understanding of bubbly cloud cavitation. It has become clear that effects due to the interaction between bubbles may be crucially important especially when they give rise to the phenomenon called cloud cavitation. Calculations of the growth and collapse of a spherical cloud of cavitating bubbles show that when the cloud interaction parameter ( $\beta$ ) is large enough, collapse occurs first on the surface of the cloud. As was anticipated by the work of Mørch, Kedrinskii and Hanson (Mørch 1980, 1981, 1982 and Hanson *et al.* 1981), the inward propagating collapse front becomes a bubbly shock wave which grows in magnitude due to geometric focussing. Very large pressures and radiated impulses occur when this shock wave reaches the center of the cloud.

Of course, actual clouds are far from spherical. And, even in a homogeneous medium, gasdynamic shock focussing can be quite complex and involve significant non-linear effects (see, for example, Sturtevant and Kulkarny 1976). Nevertheless, it seems evident that once collapse is initiated on the surface of a cloud, the propagating shock will focus and produce large local pressure pulses and radiated acoustic pulses. It is not, however, clear exactly what form the foci might take in the highly non-uniform, three-dimensional bubbly environment of a cavitation cloud, for example, on a hydrofoil.

Experiments with hydrofoils experiencing cloud cavitation have shown that very large pressure pulses occur within the cloud and are radiated away from it during the collapse process. Within the cloud, these pulses can have magnitudes as large as  $10\text{bar}$  and durations of the order of  $10^{-4}\text{s}$ . This suggests a new perspective on cavitation damage and noise in flows which involve large collections of cavitation bubbles with a sufficiently large void fraction (or, more specifically, a large enough  $\beta$ ) so that the bubbles interact and collapse coherently. This view maintains that the cavitation noise and damage is generated by the formation and propagation of bubbly shock waves within the collapsing cloud. The experiments reveal several specific shock wave structures. One of these is the mechanism by which the large coherent collapse of a finite cloud of bubbles occurs. A more unexpected result was the discovery of more localized bubbly shock waves propagating within the bubbly mixture in several forms, as crescent-shaped regions and as leading edge structures. These seem to occur when the behavior of the cloud is less coherent. They produce surface loadings which are within an order of magnitude of the more coherent events and could also be responsible for cavitation damage. However, because they are more localized, the radiated noise they produce is much smaller than that due to global events.

The phenomena described are expected to be important features in a wide range of cavitating flows. However, the analytical results clearly suggest that the phenomena may depend strongly on the cloud interaction parameter,  $\beta$ . If this is the case, some very important scaling effects may occur. It is relatively easy to envision a situation in which the  $\beta$  value for some small scale model experiments is too small for cloud effects to be important but in which the prototype would be operating at a much larger  $\beta$  due to the larger cloud size (assuming the void fractions and bubble sizes are comparable). Under these circumstances, the model would not manifest the large cloud cavitation effects which could occur in the prototype.

Computational methods will play a key role in these developing studies. Not only will such methods

be needed for the prediction of these flows in practical applications (particularly to predict the noise and damage potential) but they are almost essential in building our understanding of simpler key problems and laboratory investigations.

In conclusion, these recent investigations provide new insights into the dynamics and acoustics both of individual cavitation bubbles and of clouds of bubbles. In turn, these insights suggest new ways of modifying and possibly ameliorating cavitation noise and damage.

## 5 Acknowledgements

My sincerest thanks to the graduate students and post-doctoral fellows who contributed to the results described, Luca d'Agostino, Douglas Hart, Sanjay Kumar, Beth McKenney, Yi-Chun Wang, Garrett Reisman, Fabrizio d'Auria, Mark Duttweiler, Al Preston and Keita Ando as well as to my colleague Tim Colonius. I am also most grateful for the support of the Office of Naval Research who sponsored much of the research described.

## 6 References

- Ando, K., Colonius, T. and Brennen, C.E. (2007). Bubbly cloud dynamics with a bubble size distribution. Manuscript in preparation.
- Arndt, R.E.A., Ellis, C.R. and Paul, S. (1993). Preliminary investigation of the use of air injection to mitigate cavitation erosion. *Proc. ASME Symp. on Bubble Noise and Cavitation Erosion in Fluid Systems*, **FED-176**, 105–116.
- Bark, G. (1985). Developments of Distortions in Sheet Cavitation on Hydrofoils. *Proc. ASME Int. Symp. on Jets and Cavities*, 470–493.
- Bark, G., and Berlekom, W.B. (1978). Experimental Investigations of Cavitation Noise. *Proc. 12th ONR Symp. on Naval Hydrodynamics*, 470–493.
- Brennen, C.E. (1995). *Cavitation and bubble dynamics*. Oxford University Press.
- Brennen, C.E., Colonius, T., d'Auria, F. and Preston, A. (1998). Computing shock waves in cloud cavitation. *Proc. CAV98 Third Int. Symp. on Cavitation, Grenoble, France*.
- Chahine, G.L. (1982). Cloud cavitation: theory. *Proc. 14th ONR Symp. on Naval Hydrodynamics*, 165–194.
- Colonius, T., Brennen, C.E. and d'Auria, F. (1998). Computation of shock waves in cavitating flows. *Proc. ASME Fluids Eng. Div. Summer Meeting, Washington, D.C.*
- d'Agostino, L. and Brennen, C.E. (1983). On the acoustical dynamics of bubble clouds. *ASME Cavitation and Multiphase Flow Forum*, 72–75.
- d'Agostino, L. and Brennen, C.E. (1988). Acoustical absorption and scattering cross-sections of spherical bubble clouds. *J. Acoust. Soc. of Amer.*, **84**, No.6, 2126–2134.
- d'Agostino, L. and Brennen, C.E. (1989). Linearized dynamics of spherical bubble clouds. *J. Fluid Mech.*, **199**, 155–176.
- de Lange, D.F., de Bruin, G.J. and van Wijngaarden, L. (1994). On the mechanism of cloud cavitation - experiment and modeling. *Proc. 2nd Int. Symp. on Cavitation, Tokyo*, 45–50.
- Franc, J.P., and Michel, J.M. (1988). Unsteady Attached Cavitation on an Oscillating Hydrofoil. *J. Fluid Mech.*, **193**, 171–189.

- Frost, D. and Sturtevant, B. (1986). Effects of ambient pressure on the instability of a liquid boiling explosively at the superheat limit. *ASME J. Heat Transfer*, **108**, 418–424.
- Hanson, I., Kedrinskii, V.K. and Mørch, K.A. (1981). On the dynamics of cavity clusters. *J. Appl. Phys.*, **15**, 1725–1734.
- Hart, D.P., Brennen, C.E. and Acosta, A.J. (1990). Observations of cavitation on a three dimensional oscillating hydrofoil. *ASME Cavitation and Multiphase Flow Forum*, **FED-98**, 49–52.
- Knapp, R.T. (1955). Recent investigations of the mechanics of cavitation and cavitation damage. *Trans. ASME*, **77**, 1045–1054.
- Kubota, A., Kato, H., Yamaguchi, H. and Maeda, M. (1989). Unsteady structure measurement of cloud cavitation on a foil section using conditional sampling. *ASME J. Fluids Eng.*, **111**, 204–210.
- Kubota, A., Kato, H. and Yamaguchi, H. (1992). A new modelling of cavitating flows - a numerical study of unsteady cavitation on a hydrofoil section. *J. Fluid Mech.*, **240**, 59–96.
- Kumar, S. and Brennen, C.E. (1991). Non-linear effects in the dynamics of clouds of bubbles. *J. Acoust. Soc. Am.*, **89**, 707–714.
- Kumar, S. and Brennen, C.E. (1992). Harmonic cascading in bubble clouds. *Proc. Int. Symp. on Propulsors and Cavitation, Hamburg*, 171–179.
- Kumar, S. and Brennen, C.E. (1993). Some nonlinear interactive effects in bubbly cavitation clouds. *J. Fluid Mech.*, **253**, 565–591.
- Le, Q., Franc, J. M. & Michel, J. M. (1993). Partial cavities: global behaviour and mean pressure distribution. *ASME J. Fluids Eng.* **115**, 243–248.
- McKenney, E.A. and Brennen, C.E. (1994). On the dynamics and acoustics of cloud cavitation on an oscillating hydrofoil. *Proc. ASME Symp. on Cavitation and Gas-Liquid Flows in Fluid Machinery and Devices*, **FED-190**, 195-202.
- Mørch, K.A. (1980). On the collapse of cavity cluster in flow cavitation. *Proc. First Int. Conf. on Cavitation and Inhomogenities in Underwater Acoustics, Springer Series in Electrophysics*, **4**, 95–100.
- Mørch, K.A. (1981). Cavity cluster dynamics and cavitation erosion. *Proc. ASME Cavitation and Polyphase Flow Forum*, 1–10.
- Mørch, K.A. (1982). Energy considerations on the collapse of cavity cluster. *Appl. Sci. Res.*, **38**, 313.
- Morgan, W.B. (1991). *Personal communication*.
- Omta, R. (1987). Oscillations of a cloud of bubbles of small and not so small amplitude. *J. Acoust. Soc. Am.*, **82**, 1018–1033.
- Petroff, C. (1993). The interaction of breaking solitary waves with an armored bed. *Ph.D. Thesis, Calif. Inst. of Tech.*
- Rambod, E., Beizaie, M., Shusser, M., Milo, S. and Gharib, M. (1999). A physical model describing the mechanism for formation of gas microbubbles in patients with mitral mechanical heart valves. *Ann. Biomed. Eng.*, **27**, 774–792.
- Reisman, G.E., McKenney, E.A. and Brennen, C.E. (1994). Cloud cavitation on an oscillating hydrofoil. *Proc. 20th ONR Symp. on Naval Hydrodynamics*, 78–89.

- Reisman, G.E., Duttweiler, M.E. and Brennen, C.E. (1997). Effect of air injection on the cloud cavitation of a hydrofoil. *Proc. ASME Fluids Eng. Div. Summer Meeting*, Paper No. FEDSM97-3249.
- Reisman, G.E., Wang, Y.-C. and Brennen, C.E. (1998). Observations of shock waves in cloud cavitation. *J. Fluid Mech.*, **355**, 255–283.
- Shen, Y., and Peterson, F.B. (1978). Unsteady Cavitation on an Oscillating Hydrofoil. *Proc. 12th ONR Symposium on Naval Hydrodynamics*, 362–384.
- Shen, Y., and Peterson, F.B. (1980). The Influence of Hydrofoil Oscillation on Boundary Layer Transition and Cavitation Noise. *Proc. 13th ONR Symposium on Naval Hydrodynamics*, 221–241.
- Soyama, H., Kato, H., and Oba, R. (1992). Cavitation Observations of Severely Erosive Vortex Cavitation Arising in a Centrifugal Pump. *Proc. Third IMechE Int. Conf. on Cavitation*, 103–110.
- Sturtevant, B. and Kulkarny, V.J. (1976). The Focusing of Weak Shock Waves. *J. Fluid Mech.*, **73**, 651–680.
- Tanguay, M. and Colonius, T. (2002). Numerical investigation of bubble cloud dynamics in shock wave lithotripsy. *Proc. ASME Fluids Eng. Div. Summer Meeting*, FEDSM2002-31010.
- Ukon, Y. (1986). Cavitation characteristics of a finite swept wing and cavitation noise reduction due to air injection. *Proc. Int. Symp. on Propeller and Cavitation*, 383–390.
- van Wijngaarden, L. (1964). On the collective collapse of a large number of gas bubbles in water. *Proc. 11th Int. Conf. Appl. Mech.*, Springer-Verlag, Berlin, 854–861.
- Wade, R.B. and Acosta, A.J. (1966). Experimental Observations on the Flow Past a Plano-Convex Hydrofoil. *ASME J. Basic Eng.*, **88**, 273–283.
- Wang, Y.-C. and Brennen, C.E. (1995a). The noise generated by the collapse of a cloud of cavitation bubbles. *Proc. ASME/JSME Symp. on Cavitation and Gas-Liquid Flow in Fluid Machinery and Devices*, **FED-226**, 17–29.
- Wang, Y.-C. and Brennen, C.E. (1995b). Shock wave and noise in the collapse of a cloud of cavitation bubbles. *Proc. 20th Int. Symp. on Shock Waves*, 1213–1218.
- Wang, Y.-C. and Brennen, C.E. (1998). One-dimensional bubbly cavitating flows through a converging-diverging nozzle. *ASME J. Fluids Eng.*, **121**, 872–880.
- Wang, Y.-C. (1999). Effects of nuclei size distribution on the dynamics of a spherical cloud of cavitation bubbles. *ASME J. Fluids Eng.*, **121**, 881–886.